ACS Sustainable Chemistry & Engineering

pubs.acs.org/journal/ascecg

Research Article

Rapid Solvent-Free Microcrystalline Cellulose Melt Functionalization with L-Lactide for the Fabrication of Green Poly(lactic acid) Biocomposites

Maria E. Genovese,*[,‖] Luca Puccinelli,[‖] Giorgio Mancini, Riccardo Carzino, Luca Goldoni, Valter Castelvetro, and Athanassia Athanassiou*

Cite This: *ACS Sustainable Chem. Eng.* 2022, 10, 9401−9410

Read Online

ACCESS | Metrics & More | Article Recommendations | Supporting Information

ABSTRACT: A green approach is proposed to achieve a rapid surface functionalization of microcrystalline cellulose (MCC) in 30 min by a solvent-free "grafting from" reaction of L-lactide through compression molding without the need for an inert atmosphere. A sufficient hydrophobization of the MCC surface is achieved with an amount of grafted poly(L-lactic acid) (PLLA) oligomers of 7 wt % with respect to MCC. The obtained MCC-*g*-PLLA is subsequently melt-compounded with poly(lactic acid) (PLA) through extrusion and injection molding. As a result of higher compatibility and interfacial adhesion of the functionalized filler with PLA, PLA/MCC-*g*-PLLA biocomposites with a cellulose content ranging from 4 to 20 wt % exhibit an enhancement in important physicochemical properties (*i.e.*, water vapor barrier, crystallinity, stiffness) compared to both pure PLA and formulations containing an equal or higher amount of nonfunctionalized MCC. At the same time, the materials retain the mechanical strength and resistance to thermal degradation of PLA. The physicochemical characteristics, excellent biocompatibility, and biodegradability of PLA and cellulose and the simplicity, rapidity, and cost-effectiveness of the grafting process render these biocomposites suitable for several applications within the plastics domain including packaging, agriculture, automotive, consumer goods, and household appliances.

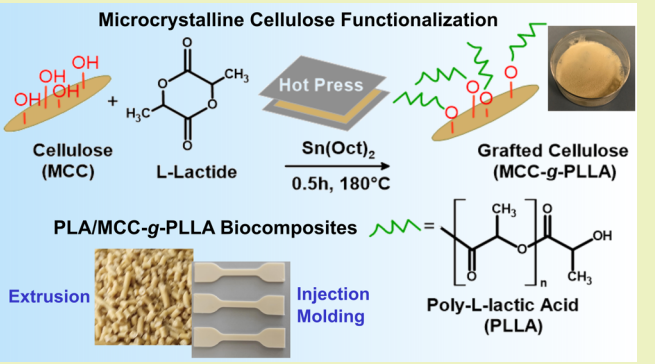

KEYWORDS: *cellulose, poly(lactic acid), melt compounding, grafting from, ring-opening polymerization, biocomposites*

INTRODUCTION

In recent years, great research efforts have been directed toward replacing fossil-based plastics with more sustainable alternatives from renewable resources to reduce the environmental impact of plastics. Among them, poly(lactic acid) (PLA), a bio-based aliphatic polyester, is one of the most attractive bioplastics of interest to researchers and industry.[1−4] The current world production of PLA is around 240,000 tons per year and is expected to double by 2023.[3] PLA has gained commercial significance, as it combines high mechanical strength, biodegradability, and good melt processability by conventional techniques used for thermoplastics, such as extrusion, injection molding, and thermoforming.[3,5] On the other hand, the industrial applications of PLA are narrowed by its relatively high cost, brittleness, slow crystallization rate, and poor barrier properties.[6,7] Several biocomposites of PLA with natural fillers have been developed recently to overcome the drawbacks of PLA, while reducing the material cost.[5,8−13] In particular, cellulose, a linear polysaccharide consisting of D-glucose units connected by *β*-1,4-D-glycosidic bonds, is the most abundant natural biopolymer. Due to its renewability, biodegradability, high availability, mechanical strength, and low price, it represents a highly valuable filler and has been shown to improve the gas barrier, mechanical properties, crystallization, and biodegradation rates of PLA.[7,8,11,12,14−16] However, in the processing of PLA/cellulose green biocomposites, the poor interfacial adhesion between the hydrophilic cellulose filler and the hydrophobic PLA matrix coupled with the strong inter and intramolecular hydrogen bonds of cellulose often results in a nonhomogeneous filler dispersion, with a negative impact on the performance and esthetic characteristics of the final materials.[6,17,18]

To improve the interaction of cellulose with the matrix, both nonreactive and reactive cellulose surface modification have been performed. Nonreactive compatibilization relies on

Received: March 22, 2022
Revised: June 30, 2022
Published: July 13, 2022

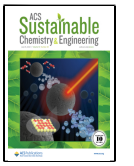

physical blending of polymers and additives bearing functional moieties that can interact with both the cellulose filler and the PLA matrix.[8,18] For instance, our group used the mildly amphiphilic poly(ethylene oxide) to promote the compatibility of cellulose fibers with PLA, obtaining an enhancement in the elongation at break by 73−143% with respect to PLA.[8] In other studies, triethyl citrate, poly(ethylene glycol), and casein were reported as effective compatibilizers.[10,19,20] However, in such systems, the intermolecular interactions (*i.e.*, dipolar, hydrogen bond, and van der Waals) are relatively weak. This possibly results in the exudation of the loosely bound components, with subsequent property changes in the material upon aging, a concern for applications such as food packaging.[21] On the other hand, the use of reactive coupling agents or the chemical modification of the cellulose surface (*e.g.*, silanization, etherification, amidation, and graft polymerization) have been proved to be more efficient at compatibilization, and thereby in material properties enhancement compared to both neat PLA and to biocomposites with nonfunctionalized cellulose. This is most likely due to the formation of stable covalent bonds and due to the presence of functional groups tailored to increase the filler/matrix interfacial compatibility.[14,18,22−28] In particular, grafting cellulose with a PLA oligomer or polymer chains through surface-initiated ring-opening polymerization (SI-ROP) is a well-established compatibilization method, in which the polysaccharide hydroxyl groups act as initiating sites along with a metal-based or an organic catalyst for the polymerization of the lactide monomer.[6,26,29−33] Most works investigated the grafting of nanostructured cellulose fillers isolated through complex, expensive, and prolonged chemical, mechanical, or enzymatic procedures that render their large-scale production challenging and result in variable morphologies and surface chemistries.[6,26,30−33] Alternatively, a limited number of studies have addressed PLA grafting of bulk or microstructured cellulose substrates, which are commercially available and less expensive compared to their nanometric counterparts.[17,25,34] For example, Guo et al. obtained microcrystalline cellulose (MCC) grafted with PLA by dissolving MCC in an ionic liquid and reacting it with L-lactide and 0.2 wt % tin octanoate as the catalyst at 110−130 °C under N_2 for 8 h.[34] In another work, MCC was functionalized by melt polycondensation of lactic acid using $SnCl_2$ as the catalyst.[35] The reaction was carried out at 130−160 °C for 2−4 h under reduced pressure after a 2 h dehydration step at 100−130 °C under vacuum. MCC was pretreated with sodium hydroxide to render it more accessible for the reaction, while Soxhlet extraction for 24 h in toluene followed by several washing steps was necessary to obtain the purified product. PLA biocomposites with 2−4 wt % of the modified filler exhibited an enhanced melt strength and crystallization rate with respect to PLA, but the data were not compared to biocomposites with unmodified MCC to assess the effect of grafting. Finally, Xiao et al. proposed a similar MCC grafting method with a reaction time of 12 h at 60−150 °C followed by Soxhlet extraction for 48 h.[36] The filler was then compounded with PLA by melt mixing and subsequent compression molding and exhibited a higher mechanical strength compared to pure PLA and to samples loaded with untreated MCC. Overall, the above methods appear impractical and not sustainable both in terms of cost and environmental impact, as they require long reaction times, the use of organic solvents and of an inert atmosphere, and extensive pre- and post-treatments with associated industrial challenges. Additionally, environmental hazards may originate from the chemicals used in the process and from the large amounts of liquid waste to dispose.[6,26,30−36]

To overcome such limitations by addressing both technical concerns and sustainability-related aspects, in this work, a new straightforward, fast, cost-effective, and greener alternative for the surface modification of MCC is proposed. The approach, based on a heterogeneous SI-ROP "grafting from" reaction with PLLA oligomers, is aimed at improving the compatibility of cellulosic fillers in biopolymer matrices and is functional for the preparation of PLA/MCC biocomposites with enhanced properties. Specifically, this method is more environmentally sustainable and industrially scalable with respect to previous reports, as it ensures the following advantages: (i) faster reaction times, (ii) the use of commercially available MCC fillers without any chemical pretreatment, (iii) surface MCC functionalization carried out in the melt phase of L-lactide by hot-pressing in a compression molding machine without the need for a solvent or inert atmosphere, (iv) a straightforward purification procedure, and (v) the melt compounding of the resulting modified filler with the polymer matrix using standard equipment. In particular, the hot press was previously used by our group for the melt polycondensation of aleuritic acid.[37] With this technique, the applied pressure prevents the evaporation of the monomer at the temperature used for the reaction that could result in reactivity losses and poor reaction yield. It is anticipated that, through this approach, MCC-*g*-PLLA with a good degree of hydrophobization can be obtained in only 30 min. More importantly, due to improved compatibility and adhesion with the PLA matrix, the resulting PLA biocomposites exhibit a more uniform dispersion in the polymer matrix and enhanced Young's modulus, crystallinity, and water vapor barrier with respect to PLA and to biocomposites, in which MCC is not compatibilized, with differences that depend on the filler content and on the specific property considered. Overall, the agile and green "grafting from" approach proposed can be exploited for the rapid functionalization of MCC rendering cellulose fillers suitable for melt compounding with PLA and other biopolyesters for industrially scalable production of sustainable biocomposites with suitable properties for applications in the traditional sectors of the plastics industry such as packaging, agriculture, and consumer goods.

EXPERIMENTAL SECTION

Materials. Poly(lactic acid) (PLA) Ingeo 2003D was purchased from NatureWorks LLC (Minnetonka, Minnesota). Microcrystalline cellulose (MCC), (3*S*)-*cis*-3,6-dimethyl-1,4-dioxane-2,5-dione (L-lactide), tin(II) 2-ethylhexanoate ($Sn(Oct)_2$), methanol (CH_3OH), tetrahydrofuran (THF), chloroform ($CHCl_3$), deuterated dichloromethane (CD_2Cl_2), and trifluoroacetic acid (TFA-*d*) were purchased from Sigma-Aldrich. PLA and MCC were dried at 45 °C overnight prior to processing.

Synthesis of MCC-*g*-PLLA. For the synthesis of MCC-*g*-PLLA, MCC (4 g) was dried at 45 °C overnight and then mixed with L-lactide crystals (5.33−16 g) and $Sn(Oct)_2$ catalyst (0.053−0.160 g) to obtain samples with MCC and catalyst concentration of 25−75 and 1 wt %, with respect to L-lactide. The reactions were performed at 180 °C for 5−120 min in an oven or alternatively by compression molding in a hydraulic hot press (Carver 3853, Carver Inc.) by inserting the mixture between two metal plates covered by poly(tetrafluoroethylene) (PTFE) foils, using a 1 mm metal frame, and by applying a pressure of 4 tons. After cooling to room temperature, a solid yellowish product was collected and stirred in $CHCl_3$ (0.1 g/mL) followed by centrifugation for 3−5 min at 5000 rpm to remove

https://doi.org/10.1021/acssuschemeng.2c01707
ACS Sustainable Chem. Eng. 2022, 10, 9401−9410

nongrafted PLLA oligomers and the unreacted L-lactide monomer. To determine the reaction yield under optimized conditions, after solvent evaporation, the residual unreacted L-lactide was separated from the nongrafted PLLA through precipitation in CH_3OH, resuspension in CH_3OH, centrifugation at 3000 rpm for 3 min, and drying. Control samples were obtained by mixing MCC in a $CHCl_3$ solution of PLLA oligomers and subsequent washing with $CHCl_3$, and by performing the grafting reaction with 25 wt % MCC to L-lactide with no catalyst for 2 h at 180 °C in the hot press, followed by the abovementioned purification procedure. Dispersion tests were carried out by suspending 10 mg of MCC and MCC-*g*-PLLA powders in 3 mL of a water:$CHCl_3$ 1:1 v/v solution.

Preparation of PLA/MCC and PLA/MCC-*g*-PLLA Biocomposites. PLA/MCC and PLA/MCC-*g*-PLLA biocomposites with a cellulose content ranging from 4 to 30 wt % were obtained through extrusion at 180 °C, with a screw rate of 150 rpm and a residence time of the material of ∼1 min in a single screw extruder with a length to diameter ratio (L/D) of 20 (Rheoscam, Scamex). The extruded strands were cut into 3 mm pellets and dried at 45 °C overnight. The pellets were then further processed using a micro-injection molding machine (Babyplast 6/10P, Rambaldi + Co I.T. Srl) setting the plasticization, injection chamber, and nozzle at 210, 205, and 200 °C, respectively, and the injection pressure at 100 bar to obtain prismatic dogbone specimens (75 mm × 4 mm × 2 mm). Films of PLA/MCC and PLA/MCC-*g*-PLLA biocomposites (100 mm × 100 mm × 1 mm) were obtained by compression molding at 170 °C with an applied pressure of 4 tons for 5 min by means of a hydraulic hot press (Carver 4386, Carver Inc.). The characterization reported in the following paragraphs was performed on dogbones unless otherwise stated.

Chemical Analysis. The synthesis of MCC-*g*-PLLA was monitored using a Fourier transform infrared (FTIR) spectrometer (Vertex 70v FTIR, Bruker) coupled with an attenuated total reflectance (ATR) accessory (MIRacle ATR, PIKE Technologies). The spectra were acquired accumulating 128 scans in the 4000−600 cm^{-1} spectral range with a scanning resolution of 4 cm^{-1} and were normalized at 1028 cm^{-1}, the strongest typical IR absorption of the cellulose backbone, which is not affected by the grafting reaction. The PLLA weight percentage to MCC was estimated from the absorbance of its carbonyl group at 1748 cm^{-1} through a calibration curve obtained with different physical mixtures of PLLA/MCC containing 1−12 wt % of PLLA with respect to MCC.

The chemical structure of pure MCC, MCC-*g*-PLLA, and nongrafted PLLA, as well as the molecular weight of MCC-*g*-PLLA and nongrafted PLLA, were determined by nuclear magnetic resonance (NMR). NMR was also used to calculate the degree of oligomerization (DO), the molar substitution (MS_{PLLA}), *i.e.*, the average number of introduced lactyl units per anhydroglucose residue of cellulose, and the degree of substitution (DS_{PLLA}), *i.e.*, the average number of hydroxyl groups substituted for lactyls per anhydroglucose residue of cellulose, of MCC-*g*-PLLA (see the Supporting Information file). Prior to the analysis, 10 mg of each sample was added to 1 mL of deuterated solvent system CD_2Cl_2/TFA-*d* (1:1, v/v) and placed in an ultrasonic bath set at 30 °C for 4 h. The spectra were acquired using a Bruker Avance III 600 MHz spectrometer, equipped with a 5 mm QCI cryoprobe with a *z* shielded pulsed-field gradient coil, using 5 mm tubes filled with 500 μL of the sample solution. ^{1}H NMR spectra were acquired with 64 transients, over a spectral width of 20.55 ppm (offset at 4.7 ppm), at a fixed receiver gain (1), and using 30 s of interpulse delay. ^{13}C inverse ^{1}H gated decoupled experiments were performed with 13,312 transients, over a spectral width of 239.0 ppm (offset at 100.0 ppm), using 2.5 s of inter pulses delay. A line broadening of 0.1 and 1.0 Hz respectively for ^{1}H and ^{13}C were applied to free induction decays (FIDs) before Fourier transform. All of the ^{1}H spectra were referred to the nondeuterated residual peak (*i.e.*, $CHDCl_2$) at 5.32 ppm, whereas the ^{13}C spectra were referred to the ^{13}C signal of CD_2Cl_2 in natural abundance at 54.0 ppm.

Morphology. The morphology of PLA and of the biocomposites was characterized by scanning electron microscopy (SEM) using a JEOL JSM-6490LA microscope, operating at 10 kV acceleration voltage under high vacuum. Prior to imaging, each sample was cryogenically fractured with nitrogen, to reveal its cross-sectional structure, and coated with a 10 nm thick gold layer using a Cressington 208HR sputtercoater (Cressington Scientific Instrument Ltd., U.K.).

Thermal Analysis. Thermal degradation analysis was carried out with a thermogravimetric analyzer (TGA, Q500, TA Instrument) on 7−12 mg of PLA and biocomposite samples heated from 30 to 700 °C at a heating rate of 10 °C/min under a 50 mL/min nitrogen flow. The thermal properties of the biocomposites were investigated using a differential scanning calorimetry (DSC) analyzer (TA Instruments Discovery DSC 250). For each sample (4−5 mg), a first heating scan from −20 to 200 °C, followed by cooling to −20 °C and a second heating to 200 °C at a rate of 10 °C/min were performed, with isotherms at 200 and −20 °C for 1 min between each scan. The crystallinity χ_c of the biocomposites was calculated according to eq 1[36]

$$\chi_c = \frac{\Delta H_c}{\omega_{PLA} \times \Delta H_c^\circ} \times 100\% \quad (1)$$

where χ_c is the crystallinity percentage of the composite, ΔH_c is the crystallization enthalpy calculated from the DSC integral area of the crystallization peak, ω_{PLA} is the weight fraction of the PLA matrix in the biocomposite, and ΔH_c° = 93.7 J/g is the theoretical crystallization enthalpy for a 100% crystalline PLA.[36]

Mechanical Properties. Uniaxial tensile tests of PLA and of biocomposites were performed using a universal testing system (Instron 3365), equipped with a 500 N load cell and an extensometer. Five specimens were tested for each sample at a speed of 5 mm/min until fracture. Prior to the tests, the samples were conditioned at 23 ± 2 °C and at a relative humidity of 50 ± 5% for 48 h.

Surface Analysis. X-ray photoelectron spectroscopy (XPS) analysis was performed on the biocomposite dogbones using an electron spectrometer (Specs Lab2, Berlin, Germany), equipped with a monochromatic X-ray source (set at 1253 eV) and with a hemispherical energy analyzer (Specs Phoibos HSA3500). The applied voltage of the Mg Kα X-ray source and current were set at 12 kV and 7 mA, respectively, and the pressure in the analysis chamber was ∼1 × 10^{-9} mbar. The large area lens mode was used for both wide and narrow scans. The energy pass, the energy step, and the scan number were 100 and 30, 1 and 0.1, and 5 and 15 eV for the wide and the narrow high-resolution scans, respectively. A flood gun was used to neutralize the surface charge, having an energy of 7 eV and a filament current of 2.2 A.

An optical profilometer Zeta-20, equipped with a 10× lens was used for three-dimensional (3D) measurements over a surface of 2 mm × 2.6 mm with a resolution of 1 μm to study the surface morphology of PLA and of the biocomposites on the micrometric size scale. The profile of the samples was reconstructed from the vertical variations y_i of the diagonal of the 3D scan images, from which the R_a value was calculated through eq 2

$$R_a = \frac{1}{n}\sum_{i=1}^{n} |y_i| \quad (2)$$

Interaction with Water. The static water contact angle of PLA and biocomposites was measured by dispensing a 5 μL MilliQ water droplet using an automatic contact angle goniometer (Dataphysics Oca20). For each sample, the reported value is the average of five tests. To investigate water absorption, samples were immersed in 60 mL of water at 23 °C and weighed regularly for 2 weeks using a digital analytical balance after drying with a cloth. The measurements were performed in triplicate. Water vapor permeability tests were performed at ambient temperature in cylindrical plastic cells with an internal cavity of 1 cm in height and a diameter of 7 mm filled with milliQ water. PLA and biocomposite films obtained by compression molding with a thickness of 1 mm were inserted on the top of the cavity of each cell between two o-ring gaskets. The cells were placed in a plastic case with activated silica gel beads, so that the relative humidity gradient (ΔRH) between the inside of the cell and the storage chamber was 100%. The weight loss of permeation cells was

https://doi.org/10.1021/acssuschemeng.2c01707
ACS Sustainable Chem. Eng. 2022, 10, 9401−9410

Table 1. Reaction Conditions for the Grafting of MCC with L-lactide[a]

sample	$Sn(Oct)_2$ (wt %)	MCC (wt %)	LA/AHG (mol/mol)	time (min)	heating source	g-PLLA (%)
25−5HP	1	25	9	5	hot press	4
25−5O	1	25	9	5	oven	2.1
25−10HP	1	25	9	10	hot press	4.9
25−10O	1	25	9	10	oven	2.9
25−30HP	1	25	9	30	hot press	7
25−30O	1	25	9	30	oven	4.9
25−60HP	1	25	9	60	hot press	7.2
25−60O	1	25	9	60	oven	5
25−120HP	1	25	9	120	hot press	10.2
25−120O	1	25	9	120	oven	5.4
50−30HP	1	50	5	30	hot press	5.7
75−30HP	1	75	3	30	hot press	4.5

[a]Contents of the catalyst and MCC are reported with respect to L-lactide, the content of grafted PLLA (g-PLLA) with respect to MCC. LA/AHG refers to the molar ratio of L-lactide to the anhydro glucose unit.

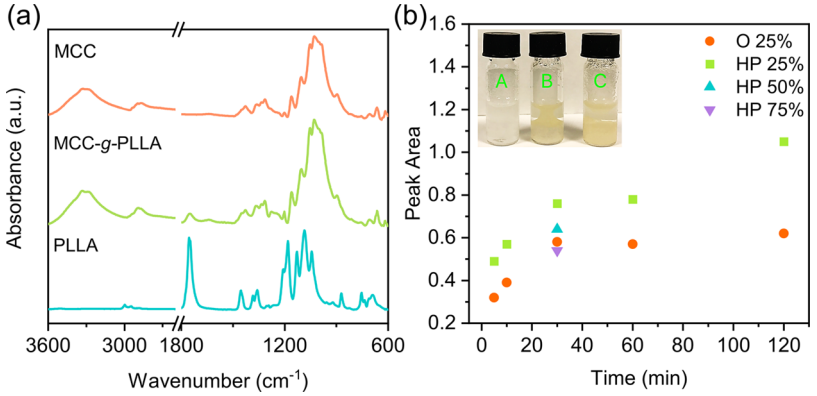

Figure 1. (a) FTIR spectra of MCC, PLA, and MCC-g-PLLA. (b) Normalized absorbance at 1748 cm^{-1} as a function of reaction conditions. Inset: dispersion tests of MCC (Vial A), MCC-g-PLLA with a peak area of 0.39 (25−10O) (Vial B), and MCC-g-PLLA with a peak area of 0.76 (sample 25−30HP) (Vial C) in a 1:1 v/v water: $CHCl_3$ solution, corresponding to the grafted PLLA to MCC content of 2.9 and 7.0 wt % respectively.

recorded for 8 h and plotted as a function of time. The water vapor transmission rate (WVTR) was obtained from the slope of each line obtained through linear regression. The water vapor permeability (WVP) was then calculated according to eq 3[10]

$$\mathrm{WVP} = \frac{\mathrm{WVTR} \times t}{A \times \mathrm{RH}} \tag{3}$$

where t is the time and A is the area of the internal cylindrical cavity.

RESULTS AND DISCUSSION

MCC Functionalization. The "grafting from" approach based on the SI-ROP of L-lactide catalyzed by $Sn(Oct)_2$ was used for the functionalization of MCC through the esterification of its hydroxylic groups without the use of a solvent, yielding MCC-g-PLLA.

In this way, PLLA oligomers could be grafted on the surface of cellulose, wherein the abundant alcoholic moieties served as initiators for the reaction, as reported in the scheme in Figure S1. Table 1 summarizes the experimental conditions used to perform the MCC grafting. The catalyst concentration was kept fixed at 1 wt % with respect to L-lactide, while the reaction time, the cellulose to L-lactide monomer ratio, and the heating source were varied to determine the optimal reaction conditions.

ATR-FTIR was used to characterize the resulting MCC-g-PLLA. As it can be seen from Figure 1a, the FTIR spectrum of MCC-g-PLLA presented all of the characteristic peaks of MCC, namely the O−H stretching band at 3600−3000 cm^{-1}, the C−H stretching at 2880 cm^{-1}, the asymmetric ring breathing mode of cellulose at 1156 cm^{-1}, and the bands at 1060 cm^{-1} and at 1018 cm^{-1} relative to the C−OH stretching vibrations of secondary and primary alcohols, respectively, indicating that cellulose did not undergo any significant thermal degradation under the reaction conditions used.[8,36] The functionalization of MCC was confirmed for all samples by the appearance of an extra peak at 1748 cm^{-1} assigned to the C═O group stretching vibrations of PLA, absent in the spectrum of pure MCC. Such results are consistent with previous reports on polymerization of PLA onto MCC.[14,34,36] Moreover, by spectral analysis of control samples, obtained by suspension of MCC in a $CHCl_3$ PLLA solution and subsequent washing or by performing the reaction without catalyst, no carbonyl peak was detected (Figure S2), demonstrating that the physisorption of PLLA oligomers chains or the L-lactide monomer onto the MCC surface was negligible and that the reaction did not occur without catalyst under the conditions used in this work.

The amount of PLLA oligomers grafted onto MCC under the different reaction conditions reported in Table 1 was calculated through a calibration curve (Figure S3) from the carbonyl stretching peak area at 1748 cm^{-1} in the FTIR spectra (Figure 1b). As it can be observed from Figure 1b, by changing the cellulose to L-lactide content from 25 to 50 and 75 wt % a decrease of ∼16 and 29% was observed in the carbonyl peak area, respectively, indicating that the optimal ratio of the MCC

https://doi.org/10.1021/acssuschemeng.2c01707
ACS Sustainable Chem. Eng. 2022, 10, 9401−9410

initiator was achieved using 25 wt %. On the other hand, the LA grafting efficiency improved in absolute values from 1.75 to 3.38% upon increasing the MCC fraction from 25 to 75 wt % of the LA feed (samples 25−30HP and 75−30HP). With respect to the reaction time, the carbonyl peak area exhibited the highest value at 120 min for all tested conditions. Peculiarly, the peak areas for 1 h and for 30 min were found to be similar. Between the two different heating sources, namely oven and hot press, the yield of grafted PLA greatly increased by 31−69% when the reaction was performed in the hot press for the same reaction times, as the monomer did not evaporate due to the application of high pressure. Dispersion tests were then performed to determine the suitable amount of grafted PLLA oligomers to achieve hydrophobization of MCC by suspending the grafted MCC samples in a mixture of water and $CHCl_3$. As it can be observed from the inset of Figure 1, unmodified MCC did not disperse in the organic phase due to its hydrophilic nature. For samples with a PLLA oligomers content below 5 wt % with respect to MCC, the MCC remained at the interface of the two solvents. For PLLA values ranging between 5 and 6 wt %, the samples were initially hydrophobic but not stable over time, while, for 7 wt % or higher, the materials were completely dispersed and stable in the $CHCl_3$ phase. From both the spectroscopic analysis and the dispersion tests, it can be concluded that the best conditions to achieve sufficient MCC hydrophobicity while at the same time minimizing the reaction time were obtained by carrying out the reaction in the hot press for 30 min with 25 wt % of MCC to L-lactide (25−30HP). However, it has to be noted that the higher LA grafting efficiency at higher MCC/LA ratios (*e.g.*, 50 and 75 wt %) may also ensure sufficient MCC hydrophobicity at longer reaction times (*e.g.*, 120 min).

For sample 25−30HP, from now defined as MCC-*g*-PLLA, the chemical structure was further confirmed by ^1H and ^{13}C NMR (Figures S4−S6, Tables S1 and S2, and relative discussion), consistent with the FTIR results and with previous studies.[36,38] Moreover, the amount of PLLA grafted was determined to be 7 wt % with respect to MCC, the total conversion of L-lactide was 90%, while the degree of oligomerization, and molecular weight of the PLLA oligomers grafted on MCC were determined to be 4 and 300 g/mol, respectively, through NMR analysis, as described in the Supporting Information. The obtained values are similar to the values of 6.22 and 425 g/mol reported by Hua et al.[35] for MCC-*g*-PLLA pretreated in NaOH and then reacted with lactic acid and $SnCl_2$ for 2 h under reduced pressure. The DS_{PLLA} and MS_{PLLA} also estimated through NMR were 0.04 and 0.16, respectively. Moreover, the surface of MCC in MCC-*g*-PLLA was hydrophobized without substantial changes in the morphology and thermal degradation (Figure S7, Table S3, and relative discussion). Although a slight decrease in the maximal degradation temperature (T_{max} = 331 °C) was observed compared to MCC (T_{max} = 334 °C) and ascribed to the presence of the PLLA oligomers,[34,35,39,40] the thermal stability of MCC-*g*-PLLA was significantly higher compared to other works.[34,35] For example, the T_{max} of MCC reported by Hua et al. after functionalization with PLLA ranged from 301.7 to 321.9 °C.[35] MCC-*g*-PLLA prepared under the optimized conditions as described above was then used as a filler in biocomposites with PLA. The resulting properties will be discussed in the next section.

Biocomposites. Green biocomposites of PLA with MCC-*g*-PLLA and nonfunctionalized MCC with a filler amount ranging from 4 to 30 wt % (Table 2) were prepared through extrusion followed by injection molding to investigate the effect of MCC modification on the compatibility with the polymer matrix and on the resulting materials' surface morphology and relevant physicochemical properties.

Table 2. Composition of PLA/MCC and PLA/MCC-*g*-PLLA Biocomposites

sample	PLA (wt %)	MCC (wt %)	MCC-*g*-PLLA (wt %)
PLA	100	0	0
PLA/MCC4	96	4	0
PLA/gMCC4	96	0	4
PLA/MCC10	90	10	0
PLA/gMCC10	90	0	10
PLA/MCC20	80	20	0
PLA/gMCC20	80	0	20
PLA/MCC30	70	30	0

The section of fractured specimens of PLA, PLA/MCC, and PLA/MCC-*g*-PLLA was inspected by SEM to investigate the effect of the cellulose filler content, dispersion, and surface modification. As observed from Figure 2a, pure PLA presented a smooth surface. Upon incorporation of cellulose, no significant inhomogeneity or phase separation could be detected in the specimens with 4 wt % filler (Figure 2b,c).

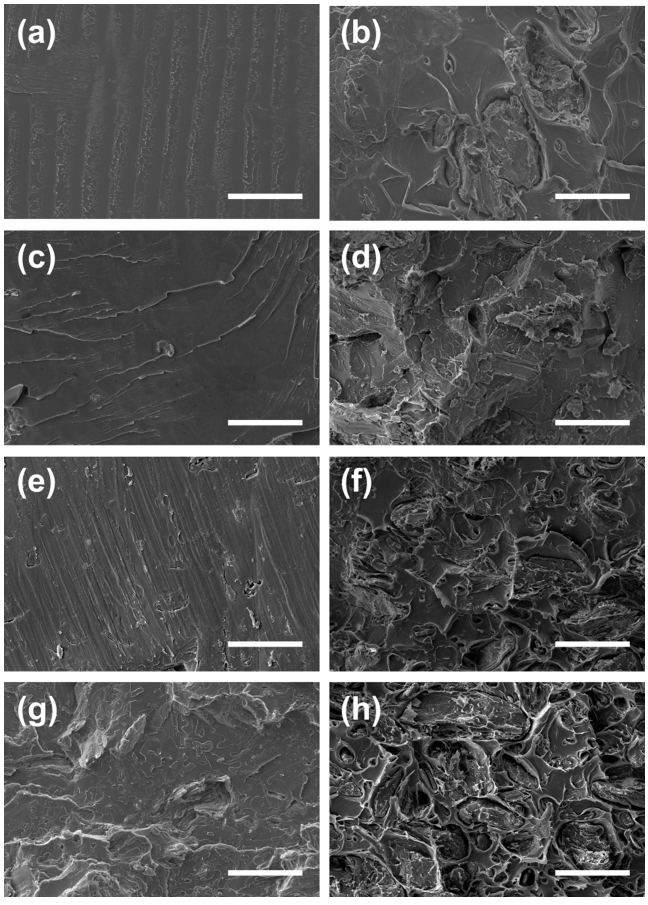

Figure 2. SEM micrographs of cryogenically fractured dogbones of (a) PLA, (b) PLA/MCC4, (c) PLA/gMCC4, (d) PLA/MCC10, (e) PLA/gMCC10, (f) PLA/MCC20, (g) PLA/gMCC20, and (h) PLA/MCC30. Scale bar = 100 μm.

https://doi.org/10.1021/acssuschemeng.2c01707
ACS Sustainable Chem. Eng. 2022, 10, 9401−9410

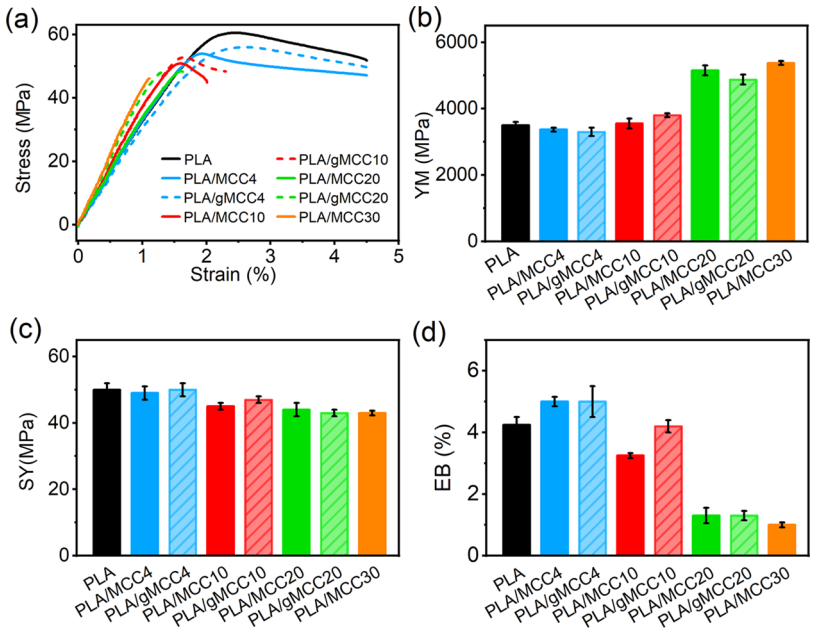

Figure 3. Stress−strain curves (a), Young's modulus (YM) (b), stress at yield (SY) (c), and elongation at break (EB) (d) of PLA, PLA/MCC, and PLA/MCC-*g*-PLLA biocomposites.

At a higher cellulose content, biocomposites with nonfunctionalized MCC (Figure 2d,f,h) presented voids and pull-outs due to a poor interfacial adhesion originating from the low compatibility with the PLA matrix.[41] In contrast, PLA/MCC-*g*-PLLA biocomposites (Figure 2c,e,g) exhibited a much more uniform filler dispersion and smoothness. This difference can be ascribed to the improved interactions of the compatibilized fillers with the matrix which lead to a more efficient stress transfer between the matrix and the filler upon fracture.[25] The biocomposites exhibited good resistance to thermal degradation, similar to pure PLA, even at high loadings of MCC, with T_{max} values ranging from 349 to 360 °C (Figure S8 and Table S4), as discussed in more detail in the Supporting Information file. In parallel, the thermal behavior and crystallinity of injection-molded pure PLA and biocomposites were investigated through DSC. As shown in Figure S9 and Table S5, the samples exhibited the characteristic PLA glass transition (T_g) at 55 °C,[40] cold crystallization (T_{cc}) between 115 and 125 °C, ascribed to the reorganization of amorphous domains in crystalline regions due to the greater macromolecular flexibility and mobility at temperatures above the glass transition (T_g)[42] and melting (T_m) between 135 and 160 °C. No crystallization was observed during cooling, due to kinetic constraints typical of PLA that require either very low crystallization rates or suitable nucleating agents to induce crystallization on cooling.[43] Specifically, the T_g and T_m did not change appreciably upon the incorporation of the cellulosic filler, while the T_{cc} of all biocomposites was lower (116−120 °C) with respect to the value registered for pure PLA (122 °C) and generally decreased as the MCC content increased, indicating that MCC acted as a nucleating agent promoting the crystallization rate of PLA.[36,44] This was further confirmed by the increase in the degree of crystallinity χ_c from 24 to 32% upon increasing the MCC content, with the highest crystallinity degree (32%) registered for the PLA/gMCC20 formulation. Most importantly, the variations in the T_{cc} and χ_c for PLA/MCC-*g*-PLLA biocomposites containing 10−20 wt % filler were greater compared not only with PLA but also with the values registered for PLA/MCC biocomposites with the same nonfunctionalized MCC content or higher, *i.e.*, 30 wt %, as a result of the improvement of the interfacial adhesion due to the compatibilization combined with the nucleating effect.[25,36] In particular, the greater the adhesion of the polymer chains to the crystal surface the lower their mobility, with a subsequent faster crystal formation.[44] Overall, the biocomposites exhibited an enhancement in the crystallinity by 12−33% with respect to pure PLA, which was generally higher compared to previous reports. For example, improvements by 1.3−12% and 3.5−14% in the crystallinity had been reported for PLA/MCC-*g*-PLLA with an MCC content of 10−30 wt %[36] and for biocomposites of PLA and 5−20 wt % MCC functionalized with a silane derivative,[18] respectively.

The effect of the MCC content and compatibilization on the mechanical properties of the materials was investigated by uniaxial tensile tests. From the mechanical parameters extracted from the relative stress/strain curves in Figure 3a−d, it can be seen that with respect to PLA Young's modulus did not substantially change for biocomposites with 4 and 10 wt % of filler, while it increased by 39−54% for biocomposites with a cellulose content of 20−30 wt % (Figure 3a,b). Such an increase in the materials' stiffness is due to the intrinsic high modulus of the rigid filler and to the increased crystallinity of the matrix.[25] The strength at yield was found to be substantially similar to that of PLA (50 ± 2 MPa), with a slight decrease of 12−14% for biocomposites with an MCC content of 20−30 wt % (Figure 3a,c). With regard to the elongation at break (Figure 3a,d), an increase was observed for an MCC content of 4 wt % (5 ± 0.15%) compared to pure PLA (4.2 ± 0.25%), while progressively lower values (1−4%) were obtained with increasing content of the MCC filler, as an effect of its low aspect ratio coupled to the weaker interaction between the poly-lactide and the crystalline cellulose chains.[36,41] Interestingly, PLA/gMCC10 exhibited a 7 and 8.6% higher modulus compared to the PLA/MCC10 biocomposite (3550 ± 150 MPa) and to pure PLA (3500 ± 100 MPa), respectively, and strength at yield (47 ± 1 MPa)

https://doi.org/10.1021/acssuschemeng.2c01707
ACS Sustainable Chem. Eng. 2022, 10, 9401−9410

and elongation at break (4.2 ± 0.2%) similar to PLA and 4.4 and 31% higher, respectively, compared with its non-functionalized counterpart (45 ± 1 MPa, 3.2 ± 0.08%), as a result of the enhanced compatibility, and thus, interfacial adhesion of the polymer matrix, which plays an important role in the stress transfer during the tensile tests. As previously suggested, the longer the grafted chains, the more easily they could create a continuous phase, in which local stresses are evenly transferred to the remaining PLA phase.[39]

On the other hand, below 10 wt % cellulose, the effect of grafting on the mechanical properties was not evident under the conditions used in this study probably due to the low amount of the filler in the polymer matrix. With regards to 20 wt % of filler, negligible differences were observed between functionalized and nonfunctionalized samples in the elongation at break and strength, while a slight decrease was detected in Young's modulus of PLA/gMCC20 (4875 ± 150 MPa) compared to PLA/MCC20 (5150 ± 150 MPa). In this case, the lack of the expected positive impact of grafting could be a result of the limited mixing effectiveness and filler dispersion that can be achieved in a single screw extruder. Such drawbacks might be overcome by melt compounding the materials using a twin screw extruder.

The wetting behavior of the biocomposites was assessed through contact angle (CA) measurements. As shown in Figure S10, the water CA values were found to increase from 75 to 85° upon increasing the content of MCC. Such effects might be ascribed to a higher roughness imparted to the surface by the MCC filler that can lead to entrapment of air pockets underneath the water drop and within the rough features of the surfaces, resulting in an enhancement of the overall hydrophobicity, consistent with previous reports.[8,45] In this case, the hydrophilic nature of MCC did not appear to influence the CAs since the surface of the composites consists predominantly of PLA, as demonstrated by the XPS analysis (Table S6) discussed in the Supporting Information file. When comparing the biocomposites with an equal amount of filler, PLA/MCC-*g*-PLLA exhibited slightly lower CA values with respect to the PLA/MCC samples, consistent with their lower surface roughness (Figure S11 and Table S7) ascribed to the stronger interfacial adhesion of MCC-*g*-PLLA to the PLA polymer, which reduces the agglomeration as well as filler detachment from the surface.

The water absorption ability and water vapor barrier properties of the materials were determined and compared with those of pure PLA. Specifically, although increasing water and moisture absorption of PLA would accelerate its biodegradation in the compost environment,[7,41] it is also true that for commercial applications, such as packaging, PLA and its biocomposites must possess an appropriate resistance to water and humidity to ensure an adequate shelf life of the product. As expected, the water absorption of PLA at equilibrium (0.3 wt %) increased up to 2 wt % upon incorporation of hydrophilic MCC (Figure 4a). However, for PLA/MCC-*g*-PLLA samples, the values were below 1 wt % and, for 10 and 20 wt % of the filler, they were 19−25% lower compared to the corresponding PLA/MCC biocomposites, demonstrating the higher hydrophobic character imparted by PLLA grafting to the cellulose filler.

Interestingly, as shown in Figure 4b, the inclusion of MCC fillers into PLA significantly improved the water vapor barrier properties by ∼45 to 66%, most likely due to the enhanced tortuosity of the path provided by the filler particles against

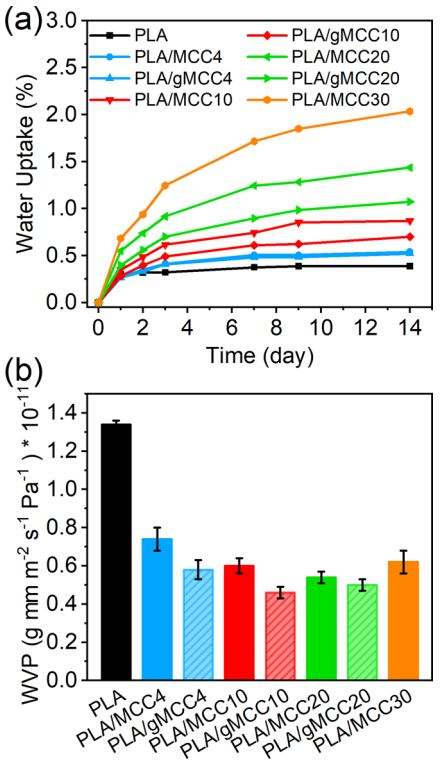

Figure 4. (a) Water absorption and (b) water vapor permeability (WVP) of PLA and of PLA/MCC and PLA/MCC-*g*-PLLA biocomposites.

permeating vapor molecules, but also, to a lesser extent, due to the observed increase in the crystallinity.[7] Generally, for the PLA/MCC-*g*-PLLA biocomposites, the WVP was found to further decrease with respect to the corresponding biocomposites with nonfunctionalized MCC due to the improved adhesion between the filler and the PLA matrix, with the lowest WVP value detected for the PLA/gMCC10 sample, as in this material an optimal dispersion and interfacial compatibilization of MCC were achieved. The obtained results are in line with previous findings.[7,46,47] For example, with respect to PLA, a decrease by 27−50% in the water vapor permeability was reported for PLA/cellulose nanocomposites[47] and a reduction by ∼47 and 66% was observed in PLA/MCC samples compatibilized with 15 and 10 wt % of triethyl citrate respectively.[10]

CONCLUSIONS

In this study, the fabrication of biodegradable and sustainable biocomposites with enhanced properties based on MCC and PLA was reported. To achieve good dispersion and improve the compatibility between the hydrophobic PLA matrix and the hydrophilic MCC filler, a green rapid one-step MCC functionalization method was developed. Specifically, PLLA oligomers were grafted on the surface of cellulose by heterogeneous SI-ROP of L-lactide "grafting from" reaction by compression molding, without the use of a solvent or inert atmosphere typical for cellulose modification. The reaction conditions were optimized to T = 180 °C, reaction time = 30 min, 25 wt % of MCC, and 1 wt % catalyst with respect to the L-lactide monomer, to achieve a cost-effective and rapid process with potential toward industrial scalability. Under such conditions, the reaction resulted in a 90% total conversion of

https://doi.org/10.1021/acssuschemeng.2c01707
ACS Sustainable Chem. Eng. 2022, 10, 9401−9410

the L-lactide monomer and yielded MCC-*g*-PLLA with short grafted PLLA oligomers (MW = 300 g/mol, DO = 4, 7 wt % to MCC) able to hydrophobize the MCC surface.

PLA/MCC-*g*-PLLA green biocomposites with 4−20 wt % filler were then obtained *via* melt extrusion followed by injection molding. In terms of morphological and physicochemical properties, relevant differences with respect to PLA were generally observed for a 10−20 wt % filler content, with an enhancement for PLA/MCC-*g*-PLLA samples compared to the corresponding PLA/MCC biocomposites with nonfunctionalized MCC due to their improved filler matrix compatibility, interfacial adhesion, and dispersion. In particular, a 12−33% increment in crystallinity was determined in the materials along with the MCC content and functionalization, as it acted as a nucleating agent for PLA without substantially affecting its thermal stability. In the mechanical performance, for an MCC-*g*-PLLA content of 10 wt %, the cellulose compatibilization exerted its maximal effect, with important differences compared to nonfunctionalized MCC and a higher Young's modulus with respect to pure PLA. Regarding the interactions with water, the hydrophobic character ascribed to the modification of MCC was very evident in the water uptake capacity of the materials, which was 19−25% lower in biocomposites with functionalized MCC compared to the others and remained <1 wt % even at a relatively high filler content. In parallel, an important reduction in the permeability by 45−66% was observed upon MCC addition. The water barrier properties were more enhanced for samples with grafted MCC, as a combined result of the increased tortuosity induced by the filler and its better interfacial adhesion and dispersion. In conclusion, the proposed agile solvent-free cellulose functionalization approach could pave the way toward the large-scale production of sustainable biocomposites alternative to fossil-based plastics with excellent biodegradability coupled to physicochemical properties suitable for several applications from packaging to automotive, agriculture, and homecare sectors.

■ ASSOCIATED CONTENT

Supporting Information

The Supporting Information is available free of charge at https://pubs.acs.org/doi/10.1021/acssuschemeng.2c01707.

SI-ROP reaction scheme and structure of MCC-*g*-PLLA; FTIR spectra of MCC from control reactions; calibration curve of PLLA/MCC mixtures; NMR spectra, SEM images, and TGA graphs of MCC, MCC-*g*-PLLA, and PLLA and relative tables and discussion; TGA, DSC, CA, XPS, surface 3D scans of PLA, and biocomposites and relative discussion (PDF)

■ AUTHOR INFORMATION

Corresponding Authors

Maria E. Genovese − *Smart Materials, Istituto Italiano di Tecnologia, 16163 Genoa, Italy;* orcid.org/0000-0003-4062-5710; Email: maria.genovese@iit.it

Athanassia Athanassiou − *Smart Materials, Istituto Italiano di Tecnologia, 16163 Genoa, Italy;* orcid.org/0000-0002-6533-3231; Email: athanassia.athanassiou@iit.it

Authors

Luca Puccinelli − *Smart Materials, Istituto Italiano di Tecnologia, 16163 Genoa, Italy; Department of Chemistry and Industrial Chemistry, University of Pisa, 56124 Pisa, Italy*

Giorgio Mancini − *Smart Materials, Istituto Italiano di Tecnologia, 16163 Genoa, Italy*

Riccardo Carzino − *Smart Materials, Istituto Italiano di Tecnologia, 16163 Genoa, Italy*

Luca Goldoni − *Analytical Chemistry Facility, Istituto Italiano di Tecnologia, 16163 Genoa, Italy*

Valter Castelvetro − *Department of Chemistry and Industrial Chemistry, University of Pisa, 56124 Pisa, Italy;* orcid.org/0000-0002-3302-7037

Complete contact information is available at: https://pubs.acs.org/10.1021/acssuschemeng.2c01707

Author Contributions

‖M.E.G. and L.P. contributed equally. The manuscript was written through contributions of all authors. All authors have given approval to the final version of the manuscript.

Notes

The authors declare no competing financial interest.

■ ACKNOWLEDGMENTS

The authors thank Dr. L. Ceseracciu and Dr. M. Salerno of the Materials Characterization Facility at the Istituto Italiano di Tecnologia for assistance with the mechanical and optical profilometry measurements, respectively, Dr. J.A. Heredia-Guerrero for help with the sample preparation for the NMR studies, Dr. L. Marini for her assistance with the thermal measurements, and Dr. T.B. Mai for a fruitful conversation.

■ REFERENCES

(1) Zych, A.; Perotto, G.; Trojanowska, D.; Tedeschi, G.; Bertolacci, L.; Francini, N.; Athanassiou, A. Super Tough Polylactic Acid Plasticized with Epoxidized Soybean Oil Methyl Ester for Flexible Food Packaging. *ACS Appl. Polym. Mater.* **2021**, *3*, 5087−5095.

(2) Sangeetha, V. H.; Deka, H.; Varghese, T. O.; Nayak, S. K. State of the Art and Future Prospectives of Poly(lactic acid) Based Blends and Composites. *Polym. Compos.* **2018**, *39*, 81−101.

(3) Zhou, L.; Ke, K.; Yang, M. B.; Yang, W. Recent Progress on Chemical Modification of Cellulose For High Mechanical-Performance Poly(lactic acid)/Cellulose Composite: A Short Review. *Compos. Commun.* **2021**, *23*, No. 100548.

(4) Kian, L. K.; Saba, N.; Jawaid, M.; Sultan, M. T. H. A Review on Processing Techniques of Bast Fibers Nanocellulose and Its Poly(Lactic Acid) (PLA) Nanocomposites. *Int. J. Biol. Macromol.* **2019**, *121*, 1314−1328.

(5) Getme, A. S.; Patel, B. A review: Bio-fiber's as Reinforcement in Composites of Polylactic Acid (PLA). *Mater. Today: Proc.* **2020**, *26*, 2116−2122.

(6) Goffin, A. L.; Raquez, J. M.; Duquesne, E.; Siqueira, G.; Habibi, Y.; Dufresne, A.; Dubois, P. From Interfacial Ring-Opening Polymerization to Melt Processing of Cellulose Nanowhisker-Filled Polylactide-Based Nanocomposites. *Biomacromolecules* **2011**, *12*, 2456−2465.

(7) Ferreira, F. V.; Dufresne, A.; Pinheiro, I. F.; Souza, D. H. S.; Gouveia, R. F.; Mei, L. H. I.; Lona, L. M. F. How Do Cellulose Nanocrystals Affect the Overall Properties of Biodegradable Polymer Nanocomposites: A Comprehensive Review. *Eur. Polym. J.* **2018**, *108*, 274−285.

(8) Singh, A. A.; Genovese, M. E.; Mancini, G.; Marini, L.; Athanassiou, A. Green Processing Route for Polylactic Acid−Cellulose Fiber Biocomposites. *ACS Sustainable Chem. Eng.* **2020**, *8*, 4128−4136.

(9) Delpouve, N.; Faraj, H.; Demarest, C.; Dontzoff, E.; Garda, M. R.; Delbreilh, L.; Berton, B.; Dargent, E. Water-Induced Breaking of

Interfacial Cohesiveness in a Poly(lactic acid)/Miscanthus Fibers Biocomposite. *Polymers* **2021**, *13*, 2285.
(10) Paul, U. C.; Fragouli, D.; Bayer, I. S.; Zych, A.; Athanassiou, A. Effect of Green Plasticizer on the Performance of Microcrystalline Cellulose/Polylactic Acid Biocomposites. *ACS Appl. Polym. Mater.* **2021**, *3*, 3071−3081.
(11) Xu, L.; Zhao, J.; Qian, S.; Zhu, X.; Takahashi, J. Green-Plasticized Poly(Lactic Acid)/Nanofibrillated Cellulose Biocomposites with High Strength, Good Toughness and Excellent Heat Resistance. *Compos. Sci. Technol.* **2021**, *203*, No. 108613.
(12) Qian, S.; Zhang, H.; Yao, W.; Sheng, K. Effects of Bamboo Cellulose Nanowhisker Content on the Morphology, Crystallization, Mechanical, and Thermal Properties of PLA Matrix Biocomposites. *Composites, Part B* **2018**, *133*, 203−209.
(13) Singh, A. A.; Genovese, M. E. Green and Sustainable Packaging Materials Using Thermoplastic Starch. In *Sustainable Food Packaging Technology*; Athanassiou, A., Ed.; Wiley, 2021; pp 133−160.
(14) Gupta, A.; Katiyar, V. Cellulose Functionalized High Molecular Weight Stereocomplex Polylactic Acid Biocomposite Films with Improved Gas Barrier, Thermomechanical Properties. *ACS Sustainable Chem. Eng.* **2017**, *5*, 6835−6844.
(15) Zhu, T.; Guo, J.; Fei, B.; Feng, Z.; Gu, X.; Li, H.; Sun, J.; Zhang, S. Preparation of Methacrylic Acid Modified Microcrystalline Cellulose and Their Applications in Polylactic Acid: Flame Retardancy, Mechanical Properties, Thermal Stability and Crystallization Behavior. *Cellulose* **2020**, *27*, 2309−2323.
(16) Xu, A.; Wang, Y.; Gao, J.; Wang, J. Facile Fabrication of a Homogeneous Cellulose/Polylactic Acid Composite Film with Improved Biocompatibility, Biodegradability and Mechanical Properties. *Green Chem.* **2019**, *21*, 4449−4456.
(17) Lönnberg, H.; Zhou, Q.; Brumer, H.; Teeri, T. T.; Malmström, E.; Hult, A. Grafting of Cellulose Fibers with Poly (ε-Caprolactone) and Poly (L-Lactic Acid) via Ring-Opening Polymerization. *Biomacromolecules* **2006**, *7*, 2178−2185.
(18) Li, H.; Cao, Z.; Wu, D.; Tao, G.; Zhong, W.; Zhu, H.; Qiu, P.; Liu, C. Crystallisation, Mechanical Properties and Rheological Behaviour of PLA Composites Reinforced by Surface Modified Microcrystalline Cellulose. *Plast., Rubber Compos.* **2016**, *45*, 181−187.
(19) Khakalo, A.; Filpponen, I.; Rojas, O. J. Protein-Mediated Interfacial Adhesion in Composites of Cellulose Nanofibrils and Polylactide: Enhanced Toughness Towards Material Development. *Compos. Sci. Technol.* **2018**, *160*, 145−151.
(20) Qu, P.; Gao, Y.; Wu, G.; Zhang, L. Nanocomposites of Poly (Lactic Acid) Reinforced with Cellulose Nanofibrils. *BioResources* **2010**, *5*, 1811−1823.
(21) Maharana, T.; Pattanaik, S.; Routaray, A.; Nath, N.; Sutar, A. K. Synthesis and Characterization of Poly (Lactic Acid) Based Graft Copolymers. *React. Funct. Polym.* **2015**, *93*, 47−67.
(22) Sheng, K.; Zhang, S.; Qian, S.; Fontanillo Lopez, C. High-Toughness PLA/Bamboo Cellulose Nanowhiskers Bionanocomposite Strengthened with Silylated Ultrafine Bamboo-Char. *Composites, Part B* **2019**, *165*, 174−182.
(23) González-López, M. E.; Robledo-Ortíz, J. R.; Manríquez-González, R.; Silva-Guzmán, J. A.; Pérez-Fonseca, A. A. Polylactic Acid Functionalization with Maleic Anhydride and Its Use as Coupling Agent in Natural Fiber Biocomposites: A Review. *Compos. Interfaces* **2018**, *25*, 515−538.
(24) Gwon, J. G.; Cho, H. J.; Chun, S. J.; Lee, S.; Wu, Q.; Lee, S. Y. Physiochemical, Optical and Mechanical Properties of Poly (Lactic Acid) Nanocomposites Filled with Toluene Diisocyanate Grafted Cellulose Nanocrystals. *RSC Adv.* **2016**, *6*, 9438−9445.
(25) Dogu, B.; Kaynak, C. Behavior of Polylactide/Microcrystalline Cellulose Biocomposites: Effects of Filler Content and Interfacial Compatibilization. *Cellulose* **2016**, *23*, 611−622.
(26) Lalanne-Tisné, M.; Mees, M. A.; Eyley, S.; Zinck, P.; Thielemans, W. Organocatalyzed Ring Opening Polymerization of Lactide From the Surface of Cellulose Nanofibrils. *Carbohydr. Polym.* **2020**, *250*, No. 116974.
(27) Qian, S.; Sheng, K. PLA Toughened by Bamboo Cellulose Nanowhisker: Role of Silane Compatibilization on the PLA Bionanocomposite Properties. *Compos. Sci. Technol.* **2017**, *148*, 59−69.
(28) Zhao, X.; Li, K.; Wang, Y.; Tekinalp, H.; Larsen, G.; Rasmussen, D.; Ginder, R. S.; Wang, L.; Gardner, D. J.; Tajvidi, M.; Webb, E.; Ozcan, S. High-Strength Polylactic Acid (PLA) Biocomposites Reinforced by Epoxy-Modified Pine Fibers. *ACS Sustainable Chem. Eng.* **2020**, *8*, 13236−13247.
(29) Gazzotti, S.; Rampazzo, R.; Hakkarainen, M.; Bussini, D.; Ortenzi, M. A.; Farina, H.; Lesma, G.; Silvani, A. Cellulose Nanofibrils as Reinforcing Agents for PLA-Based Nanocomposites: An In Situ Approach. *Compos. Sci. Technol.* **2019**, *171*, 94−102.
(30) Miao, C.; Hamad, W. Y. In-Situ Polymerized Cellulose Nanocrystals (CNC)-Poly (L-Lactide) (PLLA) Nanomaterials and Applications in Nanocomposite Processing. *Carbohyd. Polym.* **2016**, *153*, 549−558.
(31) Purnama, P.; Kim, S. H. Bio-Based Composite of Stereocomplexpolylactide and Cellulose Nanowhiskers. *Polym. Degrad. Stab.* **2014**, *109*, 430−435.
(32) Mokhena, T. C.; Sefadi, J. S.; Sadiku, E. R.; John, M. J.; Mochane, M. J.; Mtibe, A. Thermoplastic Processing of PLA/Cellulose Nanomaterials Composites. *Polymers* **2018**, *10*, 1363.
(33) Carlmark, A.; Larsson, E.; Malmström, E. Grafting of Cellulose by Ring-Opening Polymerisation-A review. *Eur. Polym. J.* **2012**, *48*, 1646−1659.
(34) Guo, Y.; Wang, X.; Shu, X.; Shen, Z.; Sun, R. C. Self-Assembly and Paclitaxel Loading Capacity of Cellulose-Graft-Poly (Lactide) Nanomicelles. *J. Agric. Food Chem.* **2012**, *60*, 3900−3908.
(35) Hua, S.; Chen, F.; Liu, Z. Y.; Yang, W.; Yang, M. B. Preparation of Cellulose-Graft-Polylactic Acid via Melt Copolycondensation for Use in Polylactic Acid Based Composites: Synthesis, Characterization and Properties. *RSC Adv.* **2016**, *6*, 1973−1983.
(36) Xiao, L.; Mai, Y.; He, F.; Yu, L.; Zhang, L.; Tang, H.; Yang, G. Bio-Based Green Composites with High Performance from Poly-(Lactic Acid) and Surface-Modified Microcrystalline Cellulose. *J. Mater. Chem.* **2012**, *22*, 15732−15739.
(37) Heredia-Guerrero, J. A.; Benítez, J. J.; Cataldi, P.; Paul, U. C.; Contardi, M.; Cingolani, R.; Bayer, I. S.; Heredia, A.; Athanassiou, A. All-Natural Sustainable Packaging Materials Inspired by Plant Cuticles. *Adv. Sustainable Syst.* **2017**, *1*, No. 1600024.
(38) Heredia-Guerrero, J. A.; Goldoni, L.; Benítez, J. J.; Davis, A.; Ceseracciu, L.; Cingolani, R.; Bayer, I. S.; Heinze, T.; Koshella, A.; Heredia, A.; Athanassiou, A. Cellulose-Polyhydroxylated Fatty Acid Ester-based Bioplastics with Tuning Properties: Acylation Via a Mixed Anhydride System. *Carbohydr. Polym.* **2017**, *173*, 312−320.
(39) Lizundia, E.; Fortunati, E.; Dominici, F.; Vilas, J. L.; Leòn, L. M.; Armentano, I.; Torre, L.; Kenny, J. M. PLLA-Grafted Cellulose Nanocrystals: Role of the CNC Content and Grafting on the PLA Bionanocomposite Film Properties. *Carbohydr. Polym.* **2016**, *142*, 105−113.
(40) Lizundia, E.; Vilas, J. L.; Leon, L. M. Crystallization, Structural Relaxation and Thermal Degradation in Poly (L-Lactide)/Cellulose Nanocrystal Renewable Nanocomposites. *Carbohydr. Polym.* **2015**, *123*, 256−265.
(41) Mathew, A. P.; Oksman, K.; Sain, M. Mechanical Properties of Biodegradable Composites from Poly Lactic Acid (PLA) and Microcrystalline Cellulose (MCC). *J. Appl. Polym. Sci.* **2005**, *97*, 2014−2025.
(42) Lönnberg, H.; Fogelstrom, L.; Samir, M. A. S. A.; Berglund, L.; Malmstrom, E.; Hult, A. Surface Grafting of Microfibrillated Cellulose with Poly(ε-Caprolactone)- Synthesis and Characterization. *Eur. Polym. J.* **2008**, *44*, 2991−2997.
(43) Yu, W.; Wang, X.; Ferraris, E.; Zhang, J. Melt crystallization of PLA/Talc in Fused Filament Fabrication. *Mater. Des.* **2019**, *182*, No. 108013.
(44) Gazzotti, S.; Farina, H.; Lesma, G.; Rampazzo, R.; Piergiovanni, L.; Ortenzi, M. A.; Silvani, A. Polylactide/Cellulose Nanocrystals: The

https://doi.org/10.1021/acssuschemeng.2c01707
ACS Sustainable Chem. Eng. 2022, 10, 9401−9410

In Situ Polymerization Approach to Improved Nanocomposites. *Eur. Polym. J.* **2017**, *94*, 173−184.
(45) Athanassiou, A.; Lygeraki, M. I.; Pisignano, D.; Lakiotaki, K.; Varda, M.; Mele, E.; Fotakis, C.; Cingolani, R.; Anastasiadis, S. H. Photocontrolled Variations in the Wetting Capability of Photochromic Polymers Enhanced by Surface Nanostructuring. *Langmuir* **2006**, *22*, 2329−2333.
(46) Fortunati, E.; Peltzer, M.; Armentano, I.; Jimenez, A.; Kenny, J. M. Combined Effects of Cellulose Nanocrystals and Silver Nanoparticles on the Barrier and Migration Properties of PLA Nano-Biocomposites. *J. Food Eng.* **2013**, *118*, 117−124.
(47) Dhar, P.; Gaur, S. S.; Soundararajan, N.; Gupta, A.; Bhasney, S. M.; Milli, M.; Kumar, A.; Katiyar, V. Reactive Extrusion of Polylactic Acid/Cellulose Nanocrystal Films for Food Packaging Applications: Influence of Filler Type on Thermomechanical, Rheological, and Barrier properties. *Ind. Eng. Chem. Res.* **2017**, *56*, 4718−4735.

https://doi.org/10.1021/acssuschemeng.2c01707
ACS Sustainable Chem. Eng. 2022, 10, 9401−9410